

Evidence for B semileptonic decays into the charmed baryon Λ_c^+

The *BABAR* Collaboration

October 27, 2018

Abstract

We present the first evidence for B semileptonic decays into the charmed baryon Λ_c^+ based on 420 fb^{-1} of data collected at the $\Upsilon(4S)$ resonance with the *BABAR* detector at the PEP-II e^+e^- storage rings. Events are tagged by fully reconstructing one of the B mesons in a hadronic decay mode. We measure the relative branching fraction $\mathcal{B}(\bar{B} \rightarrow \Lambda_c^+ X \ell^- \bar{\nu}_\ell) / \mathcal{B}(\bar{B} \rightarrow \Lambda_c^+ / \bar{\Lambda}_c^- X) = (3.2 \pm 0.9_{\text{stat.}} \pm 0.9_{\text{syst.}})\%$. The significance of the signal including the systematic uncertainty is 4.9 standard deviations.

Submitted to the 34th International Conference on High-Energy Physics, ICHEP 08,
29 July—5 August 2008, Philadelphia, Pennsylvania.

Stanford Linear Accelerator Center, Stanford University, Stanford, CA 94309

Work supported in part by Department of Energy contract DE-AC03-76SF00515.

The *BABAR* Collaboration,

B. Aubert, M. Bona, Y. Karyotakis, J. P. Lees, V. Poireau, E. Prencipe, X. Prudent, V. Tisserand
*Laboratoire de Physique des Particules, IN2P3/CNRS et Université de Savoie, F-74941 Annecy-Le-Vieux,
France*

J. Garra Tico, E. Grauges

Universitat de Barcelona, Facultat de Fisica, Departament ECM, E-08028 Barcelona, Spain

L. Lopez^{ab}, A. Palano^{ab}, M. Pappagallo^{ab}

INFN Sezione di Bari^a; Dipartimento di Fisica, Università di Bari^b, I-70126 Bari, Italy

G. Eigen, B. Stugu, L. Sun

University of Bergen, Institute of Physics, N-5007 Bergen, Norway

G. S. Abrams, M. Battaglia, D. N. Brown, R. N. Cahn, R. G. Jacobsen, L. T. Kerth, Yu. G. Kolomensky,
G. Lynch, I. L. Osipenkov, M. T. Ronan,¹ K. Tackmann, T. Tanabe

Lawrence Berkeley National Laboratory and University of California, Berkeley, California 94720, USA

C. M. Hawkes, N. Soni, A. T. Watson

University of Birmingham, Birmingham, B15 2TT, United Kingdom

H. Koch, T. Schroeder

Ruhr Universität Bochum, Institut für Experimentalphysik 1, D-44780 Bochum, Germany

D. Walker

University of Bristol, Bristol BS8 1TL, United Kingdom

D. J. Asgeirsson, B. G. Fulsom, C. Hearty, T. S. Mattison, J. A. McKenna

University of British Columbia, Vancouver, British Columbia, Canada V6T 1Z1

M. Barrett, A. Khan

Brunel University, Uxbridge, Middlesex UB8 3PH, United Kingdom

V. E. Blinov, A. D. Bukin, A. R. Buzykaev, V. P. Druzhinin, V. B. Golubev, A. P. Onuchin,
S. I. Serednyakov, Yu. I. Skovpen, E. P. Solodov, K. Yu. Todyshev

Budker Institute of Nuclear Physics, Novosibirsk 630090, Russia

M. Bondioli, S. Curry, I. Eschrich, D. Kirkby, A. J. Lankford, P. Lund, M. Mandelkern, E. C. Martin,
D. P. Stoker

University of California at Irvine, Irvine, California 92697, USA

S. Abachi, C. Buchanan

University of California at Los Angeles, Los Angeles, California 90024, USA

J. W. Gary, F. Liu, O. Long, B. C. Shen,¹ G. M. Vitug, Z. Yasin, L. Zhang

University of California at Riverside, Riverside, California 92521, USA

¹Deceased

V. Sharma

University of California at San Diego, La Jolla, California 92093, USA

C. Campagnari, T. M. Hong, D. Kovalskyi, M. A. Mazur, J. D. Richman

University of California at Santa Barbara, Santa Barbara, California 93106, USA

T. W. Beck, A. M. Eisner, C. J. Flacco, C. A. Heusch, J. Kroseberg, W. S. Lockman, A. J. Martinez,
T. Schalk, B. A. Schumm, A. Seiden, M. G. Wilson, L. O. Winstrom

University of California at Santa Cruz, Institute for Particle Physics, Santa Cruz, California 95064, USA

C. H. Cheng, D. A. Doll, B. Echenard, F. Fang, D. G. Hitlin, I. Narsky, T. Piatenko, F. C. Porter
California Institute of Technology, Pasadena, California 91125, USA

R. Andreassen, G. Mancinelli, B. T. Meadows, K. Mishra, M. D. Sokoloff
University of Cincinnati, Cincinnati, Ohio 45221, USA

P. C. Bloom, W. T. Ford, A. Gaz, J. F. Hirschauer, M. Nagel, U. Nauenberg, J. G. Smith, K. A. Ulmer,
S. R. Wagner
University of Colorado, Boulder, Colorado 80309, USA

R. Ayad,² A. Soffer,³ W. H. Toki, R. J. Wilson
Colorado State University, Fort Collins, Colorado 80523, USA

D. D. Altenburg, E. Feltresi, A. Hauke, H. Jasper, M. Karbach, J. Merkel, A. Petzold, B. Spaan, K. Wacker
Technische Universität Dortmund, Fakultät Physik, D-44221 Dortmund, Germany

M. J. Kobel, W. F. Mader, R. Nogowski, K. R. Schubert, R. Schwierz, A. Volk
Technische Universität Dresden, Institut für Kern- und Teilchenphysik, D-01062 Dresden, Germany

D. Bernard, G. R. Bonneau, E. Latour, M. Verderi
Laboratoire Leprince-Ringuet, CNRS/IN2P3, Ecole Polytechnique, F-91128 Palaiseau, France

P. J. Clark, S. Playfer, J. E. Watson
University of Edinburgh, Edinburgh EH9 3JZ, United Kingdom

M. Andreotti^{ab}, D. Bettoni^a, C. Bozzi^a, R. Calabrese^{ab}, A. Cecchi^{ab}, G. Cibinetto^{ab}, P. Franchini^{ab},
E. Luppi^{ab}, M. Negrini^{ab}, A. Petrella^{ab}, L. Piemontese^a, V. Santoro^{ab}
INFN Sezione di Ferrara^a; Dipartimento di Fisica, Università di Ferrara^b, I-44100 Ferrara, Italy

R. Baldini-Ferroli, A. Calcaterra, R. de Sangro, G. Finocchiaro, S. Pacetti, P. Patteri, I. M. Peruzzi,⁴
M. Piccolo, M. Rama, A. Zallo
INFN Laboratori Nazionali di Frascati, I-00044 Frascati, Italy

A. Buzzo^a, R. Contri^{ab}, M. Lo Vetere^{ab}, M. M. Macri^a, M. R. Monge^{ab}, S. Passaggio^a, C. Patrignani^{ab},
E. Robutti^a, A. Santroni^{ab}, S. Tosi^{ab}
INFN Sezione di Genova^a; Dipartimento di Fisica, Università di Genova^b, I-16146 Genova, Italy

²Now at Temple University, Philadelphia, Pennsylvania 19122, USA

³Now at Tel Aviv University, Tel Aviv, 69978, Israel

⁴Also with Università di Perugia, Dipartimento di Fisica, Perugia, Italy

K. S. Chaisanguanthum, M. Morii

Harvard University, Cambridge, Massachusetts 02138, USA

A. Adametz, J. Marks, S. Schenk, U. Uwer

Universität Heidelberg, Physikalisches Institut, Philosophenweg 12, D-69120 Heidelberg, Germany

V. Klose, H. M. Lacker

Humboldt-Universität zu Berlin, Institut für Physik, Newtonstr. 15, D-12489 Berlin, Germany

D. J. Bard, P. D. Dauncey, J. A. Nash, M. Tibbetts

Imperial College London, London, SW7 2AZ, United Kingdom

P. K. Behera, X. Chai, M. J. Charles, U. Mallik

University of Iowa, Iowa City, Iowa 52242, USA

J. Cochran, H. B. Crawley, L. Dong, W. T. Meyer, S. Prell, E. I. Rosenberg, A. E. Rubin

Iowa State University, Ames, Iowa 50011-3160, USA

Y. Y. Gao, A. V. Gritsan, Z. J. Guo, C. K. Lae

Johns Hopkins University, Baltimore, Maryland 21218, USA

N. Arnaud, J. Béquilleux, A. D’Orazio, M. Davier, J. Firmino da Costa, G. Grosdidier, A. Höcker,
V. Lepeltier, F. Le Diberder, A. M. Lutz, S. Pruvot, P. Roudeau, M. H. Schune, J. Serrano, V. Sordini,⁵
A. Stocchi, G. Wormser

*Laboratoire de l’Accélérateur Linéaire, IN2P3/CNRS et Université Paris-Sud 11, Centre Scientifique
d’Orsay, B. P. 34, F-91898 Orsay Cedex, France*

D. J. Lange, D. M. Wright

Lawrence Livermore National Laboratory, Livermore, California 94550, USA

I. Bingham, J. P. Burke, C. A. Chavez, J. R. Fry, E. Gabathuler, R. Gamet, D. E. Hutchcroft, D. J. Payne,
C. Touramanis

University of Liverpool, Liverpool L69 7ZE, United Kingdom

A. J. Bevan, C. K. Clarke, K. A. George, F. Di Lodovico, R. Sacco, M. Sigamani

Queen Mary, University of London, London, E1 4NS, United Kingdom

G. Cowan, H. U. Flaecher, D. A. Hopkins, S. Paramesvaran, F. Salvatore, A. C. Wren

*University of London, Royal Holloway and Bedford New College, Egham, Surrey TW20 0EX, United
Kingdom*

D. N. Brown, C. L. Davis

University of Louisville, Louisville, Kentucky 40292, USA

A. G. Denig M. Fritsch, W. Gradl, G. Schott

Johannes Gutenberg-Universität Mainz, Institut für Kernphysik, D-55099 Mainz, Germany

⁵Also with Università di Roma La Sapienza, I-00185 Roma, Italy

K. E. Alwyn, D. Bailey, R. J. Barlow, Y. M. Chia, C. L. Edgar, G. Jackson, G. D. Lafferty, T. J. West,
J. I. Yi

University of Manchester, Manchester M13 9PL, United Kingdom

J. Anderson, C. Chen, A. Jawahery, D. A. Roberts, G. Simi, J. M. Tuggle
University of Maryland, College Park, Maryland 20742, USA

C. Dallapiccola, X. Li, E. Salvati, S. Saremi

University of Massachusetts, Amherst, Massachusetts 01003, USA

R. Cowan, D. Dujmic, P. H. Fisher, G. Sciolla, M. Spitznagel, F. Taylor, R. K. Yamamoto, M. Zhao
*Massachusetts Institute of Technology, Laboratory for Nuclear Science, Cambridge, Massachusetts 02139,
USA*

P. M. Patel, S. H. Robertson

McGill University, Montréal, Québec, Canada H3A 2T8

A. Lazzaro^{ab}, V. Lombardo^a, F. Palombo^{ab}

INFN Sezione di Milano^a; Dipartimento di Fisica, Università di Milano^b, I-20133 Milano, Italy

J. M. Bauer, L. Cremaldi R. Godang,⁶ R. Kroeger, D. A. Sanders, D. J. Summers, H. W. Zhao
University of Mississippi, University, Mississippi 38677, USA

M. Simard, P. Taras, F. B. Viaud

Université de Montréal, Physique des Particules, Montréal, Québec, Canada H3C 3J7

H. Nicholson

Mount Holyoke College, South Hadley, Massachusetts 01075, USA

G. De Nardo^{ab}, L. Lista^a, D. Monorchio^{ab}, G. Onorato^{ab}, C. Sciacca^{ab}

*INFN Sezione di Napoli^a; Dipartimento di Scienze Fisiche, Università di Napoli Federico II^b, I-80126
Napoli, Italy*

G. Raven, H. L. Snoek

*NIKHEF, National Institute for Nuclear Physics and High Energy Physics, NL-1009 DB Amsterdam, The
Netherlands*

C. P. Jessop, K. J. Knoepfel, J. M. LoSecco, W. F. Wang

University of Notre Dame, Notre Dame, Indiana 46556, USA

G. Benelli, L. A. Corwin, K. Honscheid, H. Kagan, R. Kass, J. P. Morris, A. M. Rahimi,
J. J. Regensburger, S. J. Sekula, Q. K. Wong

Ohio State University, Columbus, Ohio 43210, USA

N. L. Blount, J. Brau, R. Frey, O. Igonkina, J. A. Kolb, M. Lu, R. Rahmat, N. B. Sinev, D. Strom,
J. Strube, E. Torrence

University of Oregon, Eugene, Oregon 97403, USA

⁶Now at University of South Alabama, Mobile, Alabama 36688, USA

G. Castelli^{ab}, N. Gagliardi^{ab}, M. Margoni^{ab}, M. Morandin^a, M. Posocco^a, M. Rotondo^a, F. Simonetto^{ab}, R. Stroili^{ab}, C. Voci^{ab}

INFN Sezione di Padova^a; Dipartimento di Fisica, Università di Padova^b, I-35131 Padova, Italy

P. del Amo Sanchez, E. Ben-Haim, H. Briand, G. Calderini, J. Chauveau, P. David, L. Del Buono, O. Hamon, Ph. Leruste, J. Ocariz, A. Perez, J. Prendki, S. Sitt

Laboratoire de Physique Nucléaire et de Hautes Energies, IN2P3/CNRS, Université Pierre et Marie Curie-Paris6, Université Denis Diderot-Paris7, F-75252 Paris, France

L. Gladney

University of Pennsylvania, Philadelphia, Pennsylvania 19104, USA

M. Biasini^{ab}, R. Covarelli^{ab}, E. Manoni^{ab},

INFN Sezione di Perugia^a; Dipartimento di Fisica, Università di Perugia^b, I-06100 Perugia, Italy

C. Angelini^{ab}, G. Batignani^{ab}, S. Bettarini^{ab}, M. Carpinelli^{ab}⁷, A. Cervelli^{ab}, F. Forti^{ab}, M. A. Giorgi^{ab}, A. Lusiani^{ac}, G. Marchiori^{ab}, M. Morganti^{ab}, N. Neri^{ab}, E. Paoloni^{ab}, G. Rizzo^{ab}, J. J. Walsh^a

INFN Sezione di Pisa^a; Dipartimento di Fisica, Università di Pisa^b; Scuola Normale Superiore di Pisa^c, I-56127 Pisa, Italy

D. Lopes Pegna, C. Lu, J. Olsen, A. J. S. Smith, A. V. Telnov

Princeton University, Princeton, New Jersey 08544, USA

F. Anulli^a, E. Baracchini^{ab}, G. Cavoto^a, D. del Re^{ab}, E. Di Marco^{ab}, R. Faccini^{ab}, F. Ferrarotto^a, F. Ferroni^{ab}, M. Gaspero^{ab}, P. D. Jackson^a, L. Li Gioi^a, M. A. Mazzoni^a, S. Morganti^a, G. Piredda^a, F. Polci^{ab}, F. Renga^{ab}, C. Voa^a

INFN Sezione di Roma^a; Dipartimento di Fisica, Università di Roma La Sapienza^b, I-00185 Roma, Italy

M. Ebert, T. Hartmann, H. Schröder, R. Waldi

Universität Rostock, D-18051 Rostock, Germany

T. Adye, B. Franek, E. O. Olaiya, F. F. Wilson

Rutherford Appleton Laboratory, Chilton, Didcot, Oxon, OX11 0QX, United Kingdom

S. Emery, M. Escalier, L. Esteve, S. F. Ganzhur, G. Hamel de Monchenault, W. Kozanecki, G. Vasseur, Ch. Yèche, M. Zito

CEA, Irfu, SPP, Centre de Saclay, F-91191 Gif-sur-Yvette, France

X. R. Chen, H. Liu, W. Park, M. V. Purohit, R. M. White, J. R. Wilson

University of South Carolina, Columbia, South Carolina 29208, USA

M. T. Allen, D. Aston, R. Bartoldus, P. Bechtle, J. F. Benitez, R. Cenci, J. P. Coleman, M. R. Convery, J. C. Dingfelder, J. Dorfan, G. P. Dubois-Felsmann, W. Dunwoodie, R. C. Field, A. M. Gabareen, S. J. Gowdy, M. T. Graham, P. Grenier, C. Hast, W. R. Innes, J. Kaminski, M. H. Kelsey, H. Kim, P. Kim, M. L. Kocian, D. W. G. S. Leith, S. Li, B. Lindquist, S. Luitz, V. Luth, H. L. Lynch, D. B. MacFarlane, H. Marsiske, R. Messner, D. R. Muller, H. Neal, S. Nelson, C. P. O'Grady, I. Ofte, A. Perazzo, M. Perl, B. N. Ratcliff, A. Roodman, A. A. Salnikov, R. H. Schindler, J. Schwiening, A. Snyder, D. Su, M. K. Sullivan, K. Suzuki, S. K. Swain, J. M. Thompson, J. Va'vra, A. P. Wagner, M. Weaver, C. A. West, W. J. Wisniewski, M. Wittgen, D. H. Wright, H. W. Wulsin, A. K. Yarritu, K. Yi, C. C. Young, V. Ziegler

Stanford Linear Accelerator Center, Stanford, California 94309, USA

⁷Also with Università di Sassari, Sassari, Italy

P. R. Burchat, A. J. Edwards, S. A. Majewski, T. S. Miyashita, B. A. Petersen, L. Wilden
Stanford University, Stanford, California 94305-4060, USA

S. Ahmed, M. S. Alam, J. A. Ernst, B. Pan, M. A. Saeed, S. B. Zain
State University of New York, Albany, New York 12222, USA

S. M. Spanier, B. J. Wogsland
University of Tennessee, Knoxville, Tennessee 37996, USA

R. Eckmann, J. L. Ritchie, A. M. Ruland, C. J. Schilling, R. F. Schwitters
University of Texas at Austin, Austin, Texas 78712, USA

B. W. Drummond, J. M. Izen, X. C. Lou
University of Texas at Dallas, Richardson, Texas 75083, USA

F. Bianchi^{ab}, D. Gamba^{ab}, M. Pelliccioni^{ab}
*INFN Sezione di Torino^a; Dipartimento di Fisica Sperimentale, Università di Torino^b, I-10125 Torino,
Italy*

M. Bomben^{ab}, L. Bosisio^{ab}, C. Cartaro^{ab}, G. Della Ricca^{ab}, L. Lanceri^{ab}, L. Vitale^{ab}
INFN Sezione di Trieste^a; Dipartimento di Fisica, Università di Trieste^b, I-34127 Trieste, Italy

V. Azzolini, N. Lopez-March, F. Martinez-Vidal, D. A. Milanes, A. Oyanguren
IFIC, Universitat de Valencia-CSIC, E-46071 Valencia, Spain

J. Albert, Sw. Banerjee, B. Bhuyan, H. H. F. Choi, K. Hamano, R. Kowalewski, M. J. Lewczuk,
I. M. Nugent, J. M. Roney, R. J. Sobie
University of Victoria, Victoria, British Columbia, Canada V8W 3P6

T. J. Gershon, P. F. Harrison, J. Ilic, T. E. Latham, G. B. Mohanty
Department of Physics, University of Warwick, Coventry CV4 7AL, United Kingdom

H. R. Band, X. Chen, S. Dasu, K. T. Flood, Y. Pan, M. Pierini, R. Prepost, C. O. Vuosalo, S. L. Wu
University of Wisconsin, Madison, Wisconsin 53706, USA

1 Introduction

The B decays to charmed baryons are not as well understood as the decays into charmed mesons. In particular, there is limited knowledge, both theoretical and experimental, about the B semileptonic decays into charmed baryons. If the charmed baryonic production is dominated by the emission of an external W boson, as in the case of the mesonic production $B \rightarrow DX$, then we can expect the rate of the semileptonic events to be about the same for the baryonic and mesonic processes:

$$\frac{\mathcal{B}(\overline{B} \rightarrow DX\ell^-\bar{\nu}_\ell)}{\mathcal{B}(\overline{B} \rightarrow D/\overline{D}X)} \sim \frac{\mathcal{B}(\overline{B} \rightarrow \Lambda_c^+ X\ell^-\bar{\nu}_\ell)}{\mathcal{B}(\overline{B} \rightarrow \Lambda_c^+/\overline{\Lambda}_c^- X)} \quad (1)$$

where $\ell = e$ or μ . For the mesonic process, the ratio is $\mathcal{B}(\overline{B} \rightarrow DX\ell^-\bar{\nu}_\ell)/\mathcal{B}(\overline{B} \rightarrow D/\overline{D}X) \approx 10\%$ [1]. If the baryonic ratio is found to be smaller than the mesonic ratio, there is a significant contribution from internal W emission in the baryonic production. The Feynman diagrams of B decays with internal and external W emissions are shown in Fig. 1.

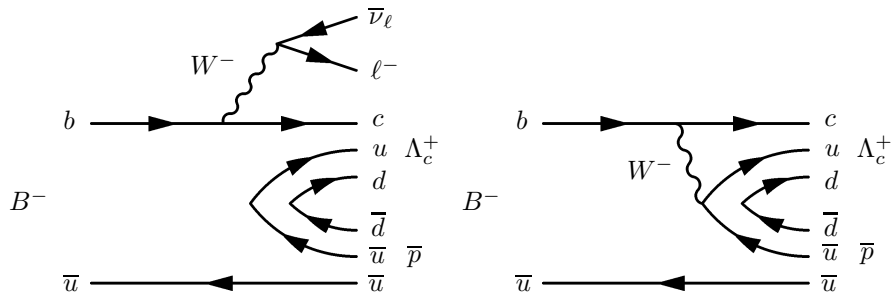


Figure 1: B decays with an external W emission (left) and an internal W emission (right).

About 90% of the inclusive semileptonic $\overline{B} \rightarrow X\ell^-\bar{\nu}_\ell$ branching fraction [2] can be accounted for by summing the branching fractions from exclusive $\overline{B} \rightarrow D^{(*)}(\pi)\ell^-\bar{\nu}_\ell$ decays. Semileptonic \overline{B} decays to charmed baryons may account for some of the remaining difference. These decays have not yet been observed. A previous search for $\overline{B} \rightarrow \Lambda_c^+ X e^-\bar{\nu}_e$ by the CLEO collaboration [3] obtained an upper limit of $\mathcal{B}(\overline{B} \rightarrow \Lambda_c^+ X e^-\bar{\nu}_e)/\mathcal{B}(\overline{B} \rightarrow \Lambda_c^+/\overline{\Lambda}_c^- X) < 0.05$ at the 90% confidence level.

In this paper, we present the first evidence for $\overline{B} \rightarrow \Lambda_c^+ X e^-\bar{\nu}_e$ decays⁸, where X can be any particle(s) from the B semileptonic decay other than the leptons and the Λ_c^+ . The $\overline{B} \rightarrow \Lambda_c^+ X e^-\bar{\nu}_e$ signal yield is obtained by a fit to the Λ_c^+ invariant mass. We perform a blind analysis using Monte-Carlo (MC) samples and the Λ_c^+ invariant mass sidebands on data to optimize the selection criteria and estimate the backgrounds. We also present the results for a similar search for $\overline{B} \rightarrow \Lambda_c^+ X \mu^-\bar{\nu}_\mu$.

2 The **BABAR** Detector and Dataset

This analysis is based on data collected with the **BABAR** detector at the PEP-II storage rings. The total integrated luminosity of the dataset is 420 fb^{-1} collected on the $\Upsilon(4S)$ resonance. The

⁸Charge-conjugate modes are implied throughout this paper.

corresponding number of produced $B\bar{B}$ pairs is roughly 460 million. An additional 42 fb^{-1} data sample taken at a center-of-mass (CM) energy 40 MeV below the $\Upsilon(4S)$ resonance is used to study background from $e^+e^- \rightarrow f\bar{f}$ ($f = u, d, s, c, \tau$) events (continuum production). The *BABAR* detector is described in detail elsewhere [4]. Charged-particle trajectories are measured by a 5-layer double-sided silicon vertex tracker and a 40-layer drift chamber, both operating in a 1.5-T magnetic field. Charged-particle identification is provided by the average energy loss (dE/dx) in the tracking devices and by an internally reflecting ring-imaging Cherenkov detector. Photons are detected by a CsI(Tl) electromagnetic calorimeter. Muons are identified by the instrumented magnetic-flux return. A detailed GEANT4-based MC simulation [5] of $B\bar{B}$ and continuum events has been used to study the detector response, its acceptance, and to test the analysis techniques.

3 Simulation of $\overline{B} \rightarrow \Lambda_c^+ X \ell^- \bar{\nu}_\ell$ Decays

Due to a lack of available theoretical models for semileptonic B decays to charmed baryons, we use an ad-hoc model to study selection optimization in our analysis. In our model, the B decays semileptonically into charmed baryons through an intermediate massive particle Y as $\overline{B} \rightarrow Y \ell^- \bar{\nu}_\ell$, according to a phase space model [6]. The Y subsequently decays into a Λ_c^+ , an anti-nucleon (anti-proton or anti-neutron), and n_1 (n_2) charged (neutral) pions, with n_1 and n_2 distributed as Poissonians with a common mean of 1.25. We apply isospin symmetry in the final states of the Y decay.

Due to the ad-hoc nature of the signal model, we tune its parameters as part of the analysis. We perform a first optimization of the selection criteria using a pseudo-particle Y mass m_Y of 4.0 GeV/c^2 and a width Γ_Y of 0.6 GeV/c^2 , with the Y decay constrained by $n_1 + n_2 \leq 4$. After unblinding the Λ_c^+ invariant mass signal region, we compare the sideband-subtracted signal distributions of the Λ_c^+ and lepton momentum spectra, and the charged and neutral pion multiplicity, with the corresponding ones from the signal MC simulation. We then tune the signal model parameters to resemble the observed distributions on data. For instance, by adjusting the mass and width of the pseudo-particle Y , we can control the shape of the lepton momentum spectrum. We find a good agreement with the electron spectrum in data for $m_Y = 4.5 \text{ GeV}/c^2$, $\Gamma_Y = 0.2 \text{ GeV}/c^2$, and $n_1 + n_2 \leq 6$. We use the retuned signal model to re-optimize the selection criteria and to estimate signal efficiency. We check *a posteriori* that the two-pass selection criteria optimization does not strongly depend on the initial signal model parameters used. The Λ_c^+ and lepton momentum spectra for a sample of signal MC events are shown in Fig. 2 for two the models before and after tuning.

4 Event Selection

We select B semileptonic decays in events containing a fully reconstructed B meson (B_{tag}), which allows us to constrain the kinematics, to reduce the combinatorial background, and to determine the charge and flavor of the signal B , up to flavor-changing mixing.

We first reconstruct the B semileptonic decay, selecting a lepton with momentum p_ℓ^* in the CM frame higher than 0.35 GeV/c . Electrons from photon conversion and π^0 Dalitz decay are removed using a dedicated algorithm, which uses a least-squares fit to reconstruct the vertex between two tracks of opposite charges whose kinematical parameters are compatible with a photon conversion or a π^0 Dalitz decay. Tracks identified as electrons or muons are required to be within 0.1 cm of the the interaction point at their point of closest approach in the transverse plane. Candidate

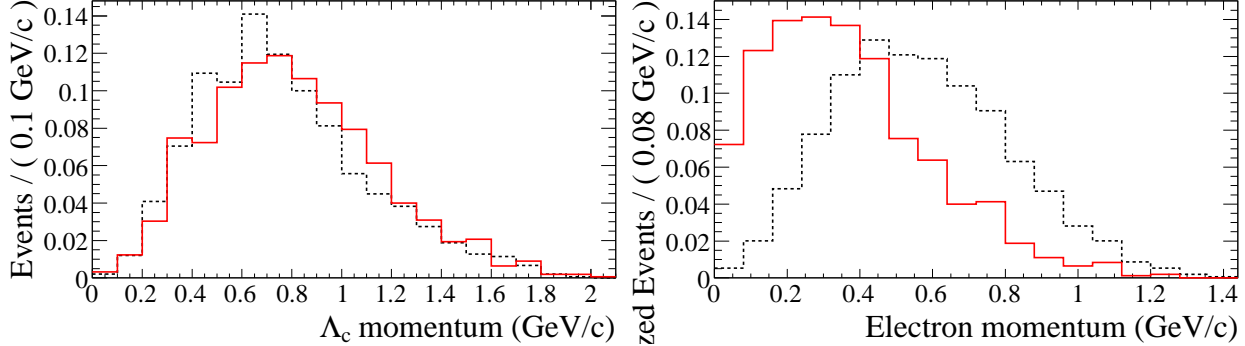


Figure 2: Λ_c^+ and lepton momentum spectra for a sample of signal MC events using the models before tuning (dashed line) and after tuning (solid line) as described in the text.

Λ_c^+ baryons, with the correct charge-flavor correlation with the lepton, are reconstructed in the $pK^-\pi^+$, pK_S^0 , $pK_S^0\pi^+\pi^-$, $\Lambda\pi^+$, $\Lambda\pi^+\pi^+\pi^-$ modes. K_S^0 (Λ) candidates are reconstructed in the $\pi^+\pi^-$ ($p\pi^-$) decay mode.

In events with multiple $\bar{B} \rightarrow \Lambda_c^+ X \ell^- \bar{\nu}_\ell$ candidates, the candidate with the highest $\Lambda_c^+ \ell^-$ vertex fit probability is selected.

We reconstruct B_{tag} decays of the type $\bar{B} \rightarrow DY'$, where Y' represents a collection of hadrons with a total charge of ± 1 , composed of $n'_1\pi^\pm + n'_2K^\pm + n'_3K_S^0 + n'_4\pi^0$, where $n'_1 + n'_2 \leq 5$, $n'_3 \leq 2$, and $n'_4 \leq 2$. Using D^0 (D^+) and D^{*0} (D^{*+}) as seeds for B^- (\bar{B}^0) decays, we reconstruct about 1000 types of decay chains. For each of the B_{tag} decay modes, the purity \mathcal{P} is estimated using MC simulation. \mathcal{P} is defined as the ratio of signal over background events with $m_{ES} \geq 5.27 \text{ GeV}/c^2$.

The kinematic consistency of a B_{tag} candidate is checked using two variables: the beam-energy substituted mass $m_{ES} = \sqrt{s/4 - \vec{p}_B^2}$, and the energy difference $\Delta E = E_B - \sqrt{s}/2$. Here \sqrt{s} refers to the total CM energy, while \vec{p}_B and E_B denote the momentum and energy of the B_{tag} candidate in the CM frame. For correctly identified B_{tag} decays, the m_{ES} distribution peaks at the B mass, while ΔE peaks at zero. We select a B_{tag} candidate in the signal region defined as $5.27 \text{ GeV}/c^2 < m_{ES} < 5.29 \text{ GeV}/c^2$, excluding B_{tag} candidates with daughter particles in common with the charmed baryon or the lepton from the B semileptonic decay.

In the case of multiple B_{tag} candidates, we select the one with the largest purity \mathcal{P} of the B_{tag} mode; in the case of multiple candidates with the same B_{tag} mode we select the one with the smallest $|\Delta E|$ value.

The B_{tag} , Λ_c^+ , and ℓ^- candidates are required to have the correct charge-flavor correlation.

By fully reconstructing one B in the event and by requiring the presence of a proton or Λ candidate, used for the Λ_c^+ reconstruction, the resulting sample shows a high purity, as is generally the case for a tagged analysis. In order to minimize model-dependent effects that can be introduced by a specific set of selection criteria, we only require the lepton momentum to be greater than $0.35 \text{ GeV}/c$, as described above, and the missing momentum to be greater than $0.2 \text{ GeV}/c$. This last cut removes background from hadronic $\bar{B} \rightarrow \Lambda_c^+ X$ decays in which all the particles in the X system have been reconstructed and one hadron is misidentified as a lepton. We also require the total charge of the reconstructed event to be zero, in order to reduce combinatorial background in the B_{tag} reconstruction from missing particles.

To obtain the B semileptonic signal yields, we perform a one-dimensional binned maximum likelihood fit to the Λ_c^+ invariant mass distribution. Backgrounds to the process of interest can

be divided according to whether they contain a correctly-reconstructed Λ_c^+ with a mass value in the signal region (peaking), and those that do not. MC studies of generic $B\bar{B}$ and continuum events show that the peaking background comes mainly from hadronic $\bar{B} \rightarrow \Lambda_c^+ X$ decays, with a fake electron from gamma conversions or π^0 Dalitz decays, or a hadron misidentified as a muon. The number of peaking background events from hadronic $\bar{B} \rightarrow \Lambda_c^+ X$ decays is estimated from the simulation, as:

$$N_{\text{peak}} = 2 \cdot \epsilon_{\text{peak}} \cdot \mathcal{B}(\bar{B} \rightarrow \Lambda_c^+ X) \cdot N_{B\bar{B}}$$

where ϵ_{peak} is the efficiency of reconstructing fake $\bar{B} \rightarrow \Lambda_c^+ X \ell^- \bar{\nu}_\ell$ events in a hadronic $\bar{B} \rightarrow \Lambda_c^+ X$ sample computed as the ratio of reconstructed and generated events, and $N_{B\bar{B}}$ is the number of $B\bar{B}$ pairs corresponding to the data luminosity. We use $\mathcal{B}(\bar{B} \rightarrow \Lambda_c^+ X) = (3.9 \pm 1.2)\%$, which is the statistical average of the charged and neutral B branching fractions [1]. We estimate $N_{\text{peak}} = 5.2 \pm 1.0_{\text{stat.}} \pm 1.7_{\text{syst.}}$ events and $N_{\text{peak}} = 15.3 \pm 1.4_{\text{stat.}} \pm 4.9_{\text{syst.}}$ events for the electron and muon samples, respectively. The sources of systematic error are described in Sec. 6.

The Λ_c^+ invariant mass distribution is fitted with the sum of three probability density functions (PDFs): one Gaussian for semileptonic $\bar{B} \rightarrow \Lambda_c^+ X \ell^- \bar{\nu}_\ell$ events, another Gaussian for peaking background events from hadronic $\bar{B} \rightarrow \Lambda_c^+ X$ decays, and a first order polynomial for combinatorial $B\bar{B}$ and continuum background events. The two Gaussians share the same mean and width, and the width is fixed to the value obtained by fitting the hadronic $\bar{B} \rightarrow \Lambda_c^+ X$ data sample, as described in Sec. 5. The amount of peaking background PDF is fixed to the MC prediction. We first fit the Λ_c^+ invariant mass sidebands, defined as the mass window of $2.23 - 2.26$, $2.31 - 2.34$ GeV/c^2 , to constrain the background PDF parameters. We then fit the Λ_c^+ invariant mass including the signal region, where the free parameters are the signal and background yields, and the Λ_c^+ mass mean value.

5 Measurement of Branching Fractions

The Λ_c^+ invariant mass distribution is compared with the results of the fit in Figure 3 for the $\bar{B} \rightarrow \Lambda_c^+ X \ell^- \bar{\nu}_\ell$ decays, where we show separately the electron and muon sample.

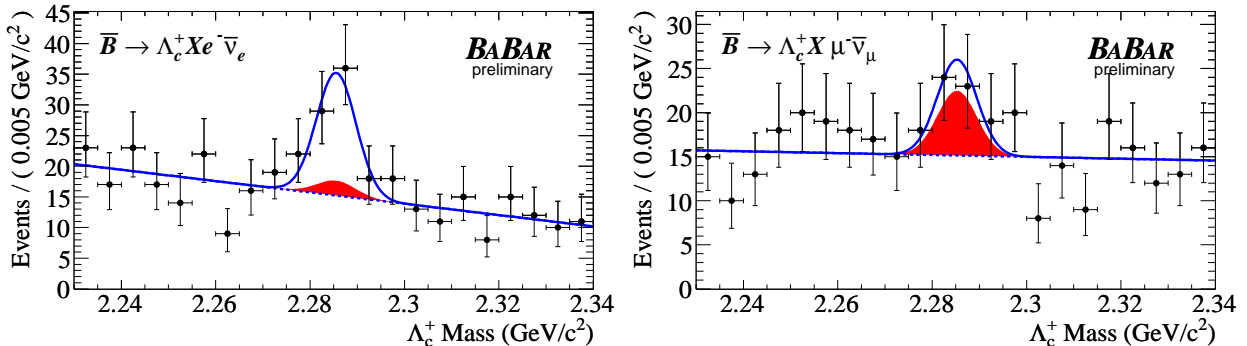


Figure 3: Fit to the Λ_c^+ distribution for $\bar{B} \rightarrow \Lambda_c^+ X e^- \bar{\nu}_e$ (left) and $\bar{B} \rightarrow \Lambda_c^+ X \mu^- \bar{\nu}_\mu$ (right): the data (points with error bars) are compared to the results of the overall fit (solid line). The peaking background contribution is shown with a shaded area. The combinatorial $B\bar{B}$ and continuum background is shown with a dashed line.

In Fig. 4 and 5, we show the distributions for the Λ_c^+ and electron momentum spectrum, and the charged and neutral pion multiplicity in the X system for the $\bar{B} \rightarrow \Lambda_c^+ X e^- \bar{\nu}_e$ sample.

These distributions are sideband-subtracted, by selecting events in the Λ_c^+ invariant mass signal region, and subtracting the combinatorial $B\bar{B}$ and continuum background using the invariant mass sidebands, and then corrected bin-by-bin by the efficiency estimated from the signal MC. The peaking background contribution is subtracted using the MC prediction.

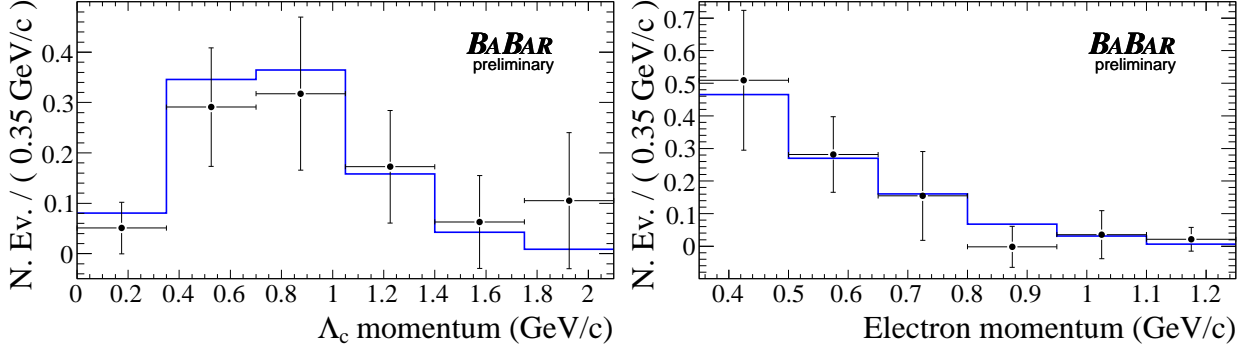


Figure 4: Sideband-subtracted, efficiency-corrected, normalized distributions for the Λ_c^+ and electron momentum spectrum in $\bar{B} \rightarrow \Lambda_c^+ X e^- \bar{\nu}_e$ decays: the data (points with error bars) are compared to the signal MC prediction.

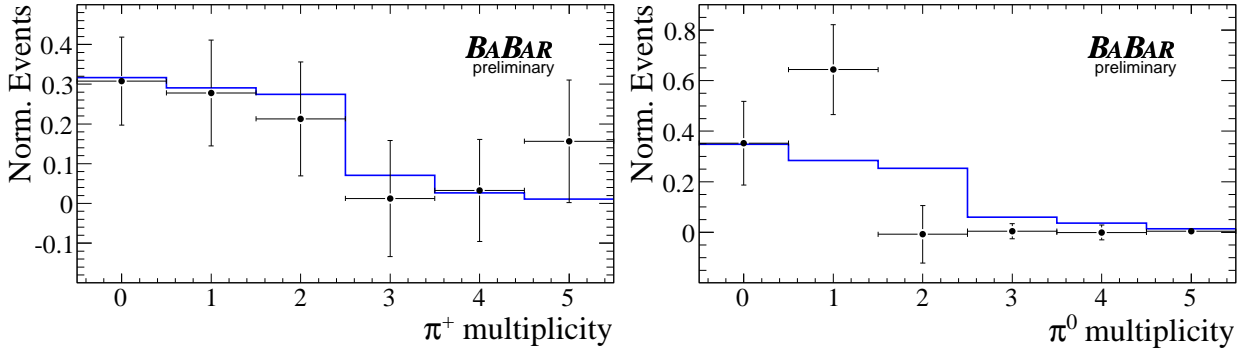


Figure 5: Sideband-subtracted, efficiency-corrected, normalized distributions for the charged and neutral pion multiplicity in the X system in $\bar{B} \rightarrow \Lambda_c^+ X e^- \bar{\nu}_e$ decays: the data (points with error bars) are compared to the signal MC prediction.

In order to reduce the systematic uncertainty, the exclusive $\mathcal{B}(\bar{B} \rightarrow \Lambda_c^+ X \ell^- \bar{\nu}_\ell)$ branching fractions are measured relative to the hadronic $\mathcal{B}(\bar{B} \rightarrow \Lambda_c^+ / \bar{\Lambda}_c^- X)$ branching fraction. To determine the hadronic branching fraction, we use a sample of $\mathcal{B}(\bar{B} \rightarrow \Lambda_c^+ / \bar{\Lambda}_c^- X)$ events selected similarly to the semileptonic channel. We select the reconstructed Λ_c^+ candidate with the highest vertex probability, and a B_{tag} candidate in the signal region defined as $5.27 \text{ GeV}/c^2 < m_{ES} < 5.29 \text{ GeV}/c^2$, excluding B_{tag} candidates with daughter particles in common with the charmed baryon. In the case of multiple B_{tag} candidates, we select the one with the largest *a priori* purity of the B_{tag} mode; in the case of multiple candidates with the same B_{tag} mode (same *a priori* purity), we select the one with the smallest $|\Delta E|$ value.

To obtain the $\bar{B} \rightarrow \Lambda_c^+ / \bar{\Lambda}_c^- X$ signal yield, we perform a one-dimensional binned maximum likelihood fit to the Λ_c^+ invariant mass distribution with the sum of two PDFs: a single Gaussian for hadronic $\bar{B} \rightarrow \Lambda_c^+ / \bar{\Lambda}_c^- X$ events, and a first order polynomial background for combinatorial

$B\bar{B}$ and continuum background events. The Λ_c^+ invariant mass distribution is compared with the results of the fit in Figure 6.

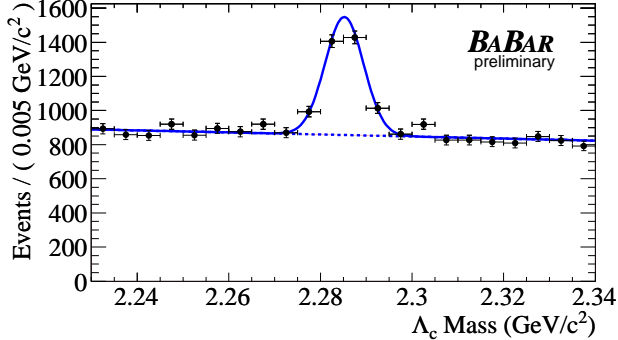


Figure 6: Fit to the Λ_c^+ distribution for $\bar{B} \rightarrow \Lambda_c^+/\bar{\Lambda}_c^- X$: the data (points with error bars) are compared to the results of the overall fit (solid line). The combinatorial $B\bar{B}$ and continuum background is shown with a dashed line.

Table 1: Signal yields and reconstruction efficiencies for the $\bar{B} \rightarrow \Lambda_c^+ X \ell^- \bar{\nu}_\ell$ and $\bar{B} \rightarrow \Lambda_c^+/\bar{\Lambda}_c^- X$ decays with statistical errors.

Decay Mode	N_{data}	$\epsilon (\times 10^{-5})$
$\bar{B} \rightarrow \Lambda_c^+ X e^- \bar{\nu}_e$	38 ± 10	2.06 ± 0.17
$\bar{B} \rightarrow \Lambda_c^+ X \mu^- \bar{\nu}_\mu$	7.4 ± 8.4	1.07 ± 0.12
$\bar{B} \rightarrow \Lambda_c^+/\bar{\Lambda}_c^- X$	1432 ± 81	3.02 ± 0.13

The relative branching fraction $\mathcal{B}(\bar{B} \rightarrow \Lambda_c^+ X \ell^- \bar{\nu}_\ell)/\mathcal{B}(\bar{B} \rightarrow \Lambda_c^+/\bar{\Lambda}_c^- X)$ is obtained by correcting the signal yields obtained from the fit by the reconstruction efficiency ratio:

$$\frac{\mathcal{B}(B \rightarrow \Lambda_c^+ X \ell^- \bar{\nu}_\ell)}{\mathcal{B}(B \rightarrow \Lambda_c^+/\bar{\Lambda}_c^- X)} = \left(\frac{N_{\text{semil}}}{N_{\text{had}}} \right) \left(\frac{\epsilon_{\text{had}}}{\epsilon_{\text{semil}}} \right).$$

Here, N_{semil} (N_{had}) is the number of $\bar{B} \rightarrow \Lambda_c^+ X$ signal events for the semileptonic (hadronic) mode, reported in Table 1 together with the corresponding reconstruction efficiencies ϵ .

6 Systematic Uncertainties

By measuring the $\bar{B} \rightarrow \Lambda_c^+ X \ell^- \bar{\nu}_\ell$ branching fraction relative to the $\bar{B} \rightarrow \Lambda_c^+/\bar{\Lambda}_c^- X$ branching fraction, many uncertainties in the reconstruction efficiency ratio cancel out. In particular, the uncertainties in the Λ_c^+ and B_{tag} reconstruction efficiencies and the Λ_c^+ decay branching fractions do not contribute.

We categorize the remaining systematic uncertainties into additive uncertainties which directly affect the signal yield, and multiplicative uncertainties which affect only the branching fraction ratio. The systematic uncertainties that have been considered are described below and summarized in Tab. 2.

Table 2: Table of systematic uncertainties. The additive errors (errors on the signal yield) are shown in units of events. The multiplicative errors (errors on the reconstruction efficiency) are shown in units of percent.

Additive systematics	$\bar{B} \rightarrow \Lambda_c^+ X e^- \bar{\nu}_e$	$\bar{B} \rightarrow \Lambda_c^+ X \mu^- \bar{\nu}_\mu$
Peaking background statistics (ev.)	1.0	1.4
Uncertainty in $\mathcal{B}(\bar{B} \rightarrow \Lambda_c^+ X)$ (ev.)	1.6	4.7
Lepton misidentification rate (ev.)	0.7	2.0
Fit bias (ev.)	0.3	1.2
Total additive (ev.)	2.0	5.4
Multiplicative systematics	$\bar{B} \rightarrow \Lambda_c^+ X e^- \bar{\nu}_e$	$\bar{B} \rightarrow \Lambda_c^+ X \mu^- \bar{\nu}_\mu$
Reconstruction efficiency statistics (%)	8.4	11.4
Model dependence (lepton momentum) (%)	22.6	71.8
Model dependence (Λ_c^+ momentum) (%)	7.5	7.5
Lepton identification efficiency (%)	1.1	2.7
Selection order (%)	3.7	44.6
Total multiplicative (%)	25.5	85.7

6.1 Additive Systematics

Systematic uncertainties in the signal yield are dominated by the peaking-background yield estimate. We evaluate this uncertainty by propagating the uncertainty in the $\bar{B} \rightarrow \Lambda_c^+ X$ branching fraction, and the Poisson error due to the limited hadronic MC statistics. We also vary the lepton misidentification probabilities by 15% for both electrons and muons, and add in quadrature the corresponding variation in the peaking background rate. To evaluate the effect of a bias in the fit technique, we perform ensembles of MC experiments, in which events are generated according to the PDF shapes measured on data, varying the signal to background rate, and fitting for the signal as in the full analysis. The difference between the fitted value of the yield and the true value is taken as a systematic error.

6.2 Multiplicative Systematics

Systematic uncertainties which affect the reconstruction efficiency ratio are dominated by the uncertainty in the signal model. To estimate this, we look for deviations in the reconstruction efficiency as we vary the tuning parameters of the signal model. The deviation in the electron spectrum is taken as the $\Delta\chi^2/\text{n.d.f.} = 1$ difference, where $\Delta\chi^2$ is the data-MC difference divided by the statistical error on data, added in quadrature for each bin of momentum, and n.d.f. = 6 is the number of bins. The deviation in the Λ_c^+ spectrum is taken as the variation in the efficiency as a function of Λ_c^+ momentum. We also include the Poisson error contribution of the limited signal MC statistics. We estimate the systematic uncertainty due to particle identification by varying the electron (muon) identification efficiency by 2% (3%). Because the event selection order is slightly different in the semileptonic and hadronic sample selections, the reconstruction efficiency systematics do not exactly cancel. We evaluate the corresponding systematic uncertainty by reversing the order of the lepton and B_{tag} selection, taking the difference in the signal yield, corrected by the reconstruction efficiency, as the systematic error. The large systematic uncertainty coming from the selection order in the muon channel is due to the low statistics of the muon sample.

7 Results

We measure the following branching ratios:

$$\frac{\mathcal{B}(B \rightarrow \Lambda_c^+ X e^- \bar{\nu}_e)}{\mathcal{B}(B \rightarrow \Lambda_c^+ / \bar{\Lambda}_c^- X)} = (3.9 \pm 1.0_{\text{stat.}} \pm 1.1_{\text{syst.}})\% \quad (2)$$

$$\frac{\mathcal{B}(B \rightarrow \Lambda_c^+ X \mu^- \bar{\nu}_\mu)}{\mathcal{B}(B \rightarrow \Lambda_c^+ / \bar{\Lambda}_c^- X)} = (1.5 \pm 1.7_{\text{stat.}} \pm 1.7_{\text{syst.}})\%. \quad (3)$$

The result for the electron channel is compatible with the CLEO result [3] of $\mathcal{B}(B \rightarrow \Lambda_c^+ X e^- \bar{\nu}_e) / \mathcal{B}(B \rightarrow \Lambda_c^+ / \bar{\Lambda}_c^- X) < 0.05$. Despite the lower value of the muon result, the two channels are compatible within their errors. Taking the weighted average of the two channels, we obtain:

$$\frac{\mathcal{B}(B \rightarrow \Lambda_c^+ X \ell^- \bar{\nu}_\ell)}{\mathcal{B}(B \rightarrow \Lambda_c^+ / \bar{\Lambda}_c^- X)} = (3.2 \pm 0.9_{\text{stat.}} \pm 0.9_{\text{syst.}})\%. \quad (4)$$

By using the hadronic branching fraction $\mathcal{B}(B \rightarrow \Lambda_c^+ / \bar{\Lambda}_c^- X) = (4.5 \pm 1.2)\%$ [1], we obtain:

$$\mathcal{B}(B \rightarrow \Lambda_c^+ X e^- \bar{\nu}_e) = (1.8 \pm 0.5_{\text{stat.}} \pm 0.7_{\text{syst.}}) \times 10^{-3} \quad (5)$$

$$\mathcal{B}(B \rightarrow \Lambda_c^+ X \mu^- \bar{\nu}_\mu) = (6.6 \pm 7.5_{\text{stat.}} \pm 7.6_{\text{syst.}}) \times 10^{-4} \quad (6)$$

$$\mathcal{B}(B \rightarrow \Lambda_c^+ X \ell^- \bar{\nu}_\ell) = (1.5 \pm 0.4_{\text{stat.}} \pm 0.6_{\text{syst.}}) \times 10^{-3}. \quad (7)$$

We evaluate the significance \mathcal{S} of our result using the log likelihood ratio $-2 \log(\mathcal{L}_{\text{max}}/\mathcal{L}_0)$ where \mathcal{L}_{max} is the maximum likelihood and \mathcal{L}_0 is the likelihood value fixing the signal yield to be zero, including statistical and systematic errors:

$$\mathcal{S}_e = \sqrt{-2 \log(\mathcal{L}_{\text{max}}/\mathcal{L}_0)} = 4.6 \quad (8)$$

$$\mathcal{S}_\mu = \sqrt{-2 \log(\mathcal{L}_{\text{max}}/\mathcal{L}_0)} = 0.8 \quad (9)$$

where the subscript e and μ denotes the electron and muon channels, respectively. The probability P that our measured signal results from a background fluctuation are computed from these \mathcal{S} values to be $P_e = 2.2 \times 10^{-6}$ and $P_\mu = 0.22$. In order to compute the significance for the combined result, we take the product of these two probabilities: $P_\ell = 4.8 \times 10^{-7}$. Converting this back to the significance, we obtain $\mathcal{S}_\ell = 4.9$ for the combined result.

In conclusion, we present the first evidence for B semileptonic decays into the charmed baryon Λ_c^+ . The relative branching fraction $\mathcal{B}(B \rightarrow \Lambda_c^+ X \ell^- \bar{\nu}_\ell) / \mathcal{B}(B \rightarrow \Lambda_c^+ / \bar{\Lambda}_c^- X)$ is found to be smaller than the corresponding one for the D charmed meson. We measure the Λ_c^+ and electron momentum spectrum in the B semileptonic decay, which could be of guidance to further development in the theoretical modeling of these decays.

8 Acknowledgments

We are grateful for the extraordinary contributions of our PEP-II colleagues in achieving the excellent luminosity and machine conditions that have made this work possible. The success of this project also relies critically on the expertise and dedication of the computing organizations that support *BABAR*. The collaborating institutions wish to thank SLAC for its support and the kind

hospitality extended to them. This work is supported by the US Department of Energy and National Science Foundation, the Natural Sciences and Engineering Research Council (Canada), the Commissariat à l’Energie Atomique and Institut National de Physique Nucléaire et de Physique des Particules (France), the Bundesministerium für Bildung und Forschung and Deutsche Forschungsgemeinschaft (Germany), the Istituto Nazionale di Fisica Nucleare (Italy), the Foundation for Fundamental Research on Matter (The Netherlands), the Research Council of Norway, the Ministry of Education and Science of the Russian Federation, Ministerio de Educación y Ciencia (Spain), and the Science and Technology Facilities Council (United Kingdom). Individuals have received support from the Marie-Curie IEF program (European Union) and the A. P. Sloan Foundation.

References

- [1] W. M. Yao *et al.* (Particle Data Group), J. Phys. **G 33**, 1 (2006) and 2007 partial update for the 2008 edition.
- [2] B. Aubert *et al.* (*BABAR* Collaboration), Phys. Rev. Lett. **100**, 151802 (2008).
- [3] G. Bonvicini *et al.* (*CLEO* Collaboration), Phys. Rev. D **57**, 6604 (1998)
- [4] B. Aubert *et al.* (*BABAR* Collaboration), Nucl. Instr. Methods Phys. Res., Sect. A **479**, 1 (2002).
- [5] S. Agostinelli *et al.*, Nucl. Instr. Methods Phys. Res., Sect. A **506**, 250 (2003).
- [6] T. Sjostrand, Comput. Phys. Commun. **82**, 74 (1994).